Integrative Biology

Accepted Manuscript

ROYAL SOCIETY OF CHEMISTRY

www.rsc.org/ibiology

Cite this: DOI: 10.1039/c0xx00000x

www.rsc.org/xxxxxx

ARTICLE TYPE

Involvement of Superoxide and Nitric Oxide in BRAFV^{600E} Inhibitor PLX4032-induced Growth Inhibition of Melanoma Cells

Ling Yu,*[a,b,c] Li Xia Gao,[a,b,c] Xiao Qing Ma,[a,b,c] Fang Xin Hu,[a,b,c] Chang Ming Li[a,b,c] and Zhisong Lu*[a,b,c]

Received (in XXX, XXX) XthXXXXXXXXX 20XX, Accepted Xth XXXXXXXXX 20XX

DOI: 10.1039/b000000x

The BRAF^{V600E} inhibitor PLX4032 (Vemurafenib) is an FDA-approved new drug for metastatic melanoma, which specifically inhibits the RAS/MEK/ERK signaling pathway to control cell proliferation and adhesion. However, no study has been carried out to investigate the role of intracellular oxidative balance in PLX4032-induced tumor growth inhibition. Herein, for the first time, superoxide ($O_2^{\cdot-}$) and nitric oxide (NO) generated from PLX4032-challenged melanoma cells were monitored with electrochemical sensors and conventional fluorescent staining techniques. Impacts of superoxide dismutase (SOD) and NG-monomethyl-L-arginine monoacetate (L-NMMA), a nitric oxide synthase inhibitor, were also examined to demonstrate the specificity of ROS/NO generation and its biological consequences. PLX4032 specifically triggers production of $O_2^{\cdot-}$ and NO from BRAF^{V600E} mutation A375 cells. SOD and L-NMMA could abolish PLX4032-induced increases in intracellular $O_2^{\cdot-}$ and NO production, thereby rescuing cell growth in BRAF mutant A375 cell (A375^{BRAFV600E}). In addition, PLX4032 treatment could decrease the mitochondrial membrane potential in A375^{BRAFV600E} cells. The results suggest that PLX4032 can selectively cause ROS production and depolarization of mitochondrial membrane, potentially initiating apoptosis and growth inhibition of PLX4032-sensitive cells. This work not only proposes a new mechanism for PLX4032-induced melanoma cell inhibition, but also highlights potential applications of electrochemical biosensors in cell biology and drug screening.

Introduction

BRAF gene encodes a serine–threonine-specific protein kinase, which plays a critical role in regulating the RAS/MEK/ERK signaling pathway.[1-3] It has been identified that mutations of *BRAF* gene are associated with human cancers, in particular human cutaneous melanoma.[4] BRAF^{V600E}, a mutation leading to the change of valine (V) to glutamate (E) at codon 600, occurs in 80% of the BRAF melanoma mutations. PLX4032 (Vemurafenib) is an inhibitor selectively targeting V600E mutation-positive BRAF kinase, demonstrating remarkable clinical activity in patients with unresectable or metastatic melanoma with BRAF^{V600E} mutations.[5, 6] It can effectively inhibit proliferation of melanoma and colon cancer cells harboring BRAF^{V600E} mutation through specifically blocking the RAS/ERK signaling pathway. [7]

Production of reactive oxygen species (ROS) is of great importance to both pathological and physiological (non-pathological) situations in human body. Overproduction of reactive free radicals may cause the formation of oxidative stress in cells, which results in severe damage to biomolecules, including lipid, protein, and DNA.[8, 9] In addition it may disrupt intracellular redox homeostasis and reduce mitochondrial membrane potential, further leading to cell death and apoptosis.[10-14] Since ROS are involved in many intracellular signaling pathways including the MAP kinase/ERKs pathway,[15, 16] they may possibly play roles in the PLX4032-induced cell inhibiting process. Corazao-Rozas *et al* examined mitochondrial metabolism in melanoma cell line that exhibits acquired resistance to PLX4032. Their study argued a therapeutic strategy by utilizing of pro-oxidants compounds because of an addiction to mitochondrial oxidative metabolism is observed in acquired inhibitor-resistant melanomas.[17] Dr. Meenhard Herlyn reported that PLX4032-treatment could lead a shift of tumor metabolism from glycolysis to oxidative phosphorylation.[18] However, the outcome of intracellular redox balance change was poorly understood.

Superoxide ($O_2^{\cdot-}$) is the major free radical that contributes to the pathogenesis of many diseases such as Alzheimer disease, myocardial infarction and atherosclerosis.[16, 19] Nitric oxide (NO) acts as an important signaling molecule in many physiological and pathological processes.[20, 21] Excessive NO may induce nitrosylation reactions to alter the structures of proteins and their normal functions.[8] Most importantly, $O_2^{\cdot-}$ and NO could react with each other to produce significant amounts of peroxynitrite (ONOO−), which is a potent oxidizing agent with high oxidative activity. [8, 22-24] Due to their biological significance, efforts have been dedicated to investigate the impact of $O_2^{\cdot-}$ and NO in

pathogenesis with different techniques such as fluorephone labeling[11, 25, 26], chemiluminescence[27] and electron spin resonance (ESR)[28]. However, those methods suffer from tedious procedures and the use of expensive instruments. Recently, electrochemical biosensor has attracted tremendous attentions due to its easy-fabrication, high sensitivity and good specificity.[29-33] Guo *et al* fabricated a layered graphene-artificial peroxidase-protein nanostructured bio-interface for *in situ* quantitative detection of ROS from cells.[32] In our previous work, DNA-$Mn_3(PO_4)_2$-carbon nanotube (CNT) nanocomposite sheets were synthesized to prepare electrochemical sensor for real-time, sensitive and specific detection of $O_2^{\cdot-}$ from tumor cells.[34] Those studies demonstrate that electrochemical biosensor is a very promising technique that can be utilized to real-time monitor local ROS concentration in solution without disturbing metabolism and the regulatory pathways of cells.

To explore the role of ROS in PLX4032-induced melanoma cell damage, for the first time, we analyzed $O_2^{\cdot-}$ and NO generation from PLX4032-treated human melanoma cell lines with electrochemical sensors. The sensing results were used together with the conventional fluorescence assays to evaluate the oxidative balance in melanoma cells harboring $BRAF^{V600E}$ mutation under the PLX4032 stimulation. Impacts of superoxide dismutase (SOD), an antioxidative enzyme, and NG-monomethyl-L-arginine monoacetate, a NO synthase inhibitor, on PLX4032-challenged melanoma cells were examined to further confirm the involvement of ROS and NO in PLX4032-caused biological consequences. The mitochondrial membrane potential was also measured to investigate the effect of PLX4032-induced oxidative stress on mitochondria.

Materials and methods

Materials

$BRAF^{V600E}$ mutate melanoma cell line A375 ($A375^{BRAFV600E}$) and $BRAF^{V600E}$ wild type melanoma cell line MV3 ($MV^{BRAFV600EWT}$) were obtained from American Type Culture Collection (ATCC). They were cultured in RPMI 1640 medium (Gibco) supplemented with 10% fetal calf serum (FCS, Gibco), 100 U ml^{-1} penicillin and 100 U ml^{-1} streptomycin at 37°C in a humidified 5% CO_2 incubator.

PLX4032, a potent inhibitor selectively targeting protein kinases with $BRAF^{V600E}$ mutation, was purchased from ChemieTek. 3-(4,5-dimethylthiazol-2-yl)-2,5-diphenyltetra- zoliumbromide (MTT), 2-(4-Amidino-phenyl)-6-indolecarb-amidinedihydro-chloride (DAPI), 3-amino,4-aminomethyl-2',7'-difluorescein diacetate (DAF-FM), dichlorodihydrofluorescin-diacetate (DCFH-DA), 5,5',6,'-tetrachloro-1,1',3,3'-tetraethylimidacarbo-cyanineiodide (JC-1), lactate dehydrogenase (LDH) cytotoxicity assay kit and NG-monomethyl-L-arginine monoacetate (L-NMMA) were purchased from Beyotime Biotechnology (Beijing, China).

All other chemicals were bought from Sigma-Aldrich and used without further purification unless otherwise indicated. All solution was prepared with deionized water produced by PURELAB flex system, ELGA Corporation.

MTT and LDH release assay

MTT cell growth assay was performed to evaluate the viability of cells under the inhibitor treatment. Briefly, $A375^{BRAFV600E}$ and $MV3^{BRAFV600E\ WT}$ cells were seeded at a density of 1×10^4/well in 96-well plates. The cells were incubated with different concentrations of PLX4032 for 72 h. After adding 10 μL MTT solution (5 mg mL^{-1}) into each well the microplates were incubated at 37° C for approximately 3–4 h. The purple-colored formazan products converted by viable cells were dissolved and measured using a spectrophotometric microplate reader ($ELx800^{TM}$, Gene Company) at 570 nm. Growth inhibition was calculated as percentage ratio between absorbance of PLX4032-treated cells and untreated cells. All experiments were performed three independent times in triplicates.

For LDH release assay, $A375^{BRAFV600E}$ and $MV3^{BRAFV600E\ WT}$ cells (1×10^4/well in 96-well plates) were stimulated with PLX4032 (5 μM) for 24, 48 and 72 h. Extracellular LDH levels were measured with the LDH cytotoxicity assay kit (Beyotime Biotechnology, China). Absorbance values were recorded at 490 nm using a microplate reader. Data were expressed as percentage of LDH enhancement in comparison with the untreated cells.

Extracellular $O_2^{\cdot-}$ and NO levels measured with electrochemical sensors

Preparation of an $O_2^{\cdot-}$ electrochemical sensor

DNA-$Mn_3(PO_4)_2$-CNT nanocomposite was synthesized according to our previous work.[34] In brief, 2.1 mg single strand DNA was added into 1 mL of 0.1 M $MnSO_4$ under constant stirring at 60°C. 9 mL 0.1 M K_3PO_4 was dropped into the mixture under stirring until the mixture becomes transparent. The pellet of DNA-$Mn_3(PO_4)_2$ composites was collected by centrifugation at 9000 rpm for 10 min. Finally, CNT (0.5 mg mL^{-1}) and DNA-$Mn_3(PO_4)_2$ (0.2 M) were drop-casted on a polished electrode.

Preparation of a NO electrochemical sensor

Reduced graphene oxide-ceria (rGO-CeO_2) nanocomposites were synthesized using a hydrothermal method. Briefly, poly-vinylpyrrolidone (0.9 g), $Ce(NO_3)_3{\cdot}6H_2O$ (0.4 g) and 500 μL graphene oxide solution (15 mg mL^{-1}) were dissolved in 30 mL deionized (DI) water, stirring for 30 min at room temperature. The mixture was transferred into a Teflon-lined autoclave and heated at 180 °C for 24 h. The obtained precipitate was collected by centrifuge at 10000 rpm for 10 minutes and then washed with ethanol and DI water. The rGO-CeO_2 nanocomposites were obtained by drying the precipitate in an oven at 70 °C for 3 h. Then rGO-CeO_2 nanocomposites were dissolved in DI water (10 mg mL^{-1}). Prior for electrode modification, the rGO-CeO_2 solution was ultrasonic treated for 1 minute. Finally, 5 μL rGO-CeO_2 nanocomposites was casted on a polished glassy carbon electrode for NO detection.

Calibration of $O_2^{\cdot-}$ and NO electrochemical sensors

A three-electrode system consisting of a nanomaterial-functionalized glassy carbon working electrode, an $Hg/HgCl_2$/KCl reference electrode and a platinum wire counter electrode was employed to electrochemically detect $O_2^{\cdot-}$ and NO on an electrochemical station (CHI 760D, Chen Hua Instruments Co. Ltd.). The electrochemical sensors were calibrated with different concentrations of $O_2^{\cdot-}$ and NO in a fluidic chamber.

Electrochemical detection of $O_2^{\cdot-}$ and NO released from cells

$A375^{BRAFV600E}$ and $MV3^{BRAFV600E\ WT}$ (5×10^5/well in a cell culture dish) cells were incubated with PLX4032 (5 μM) for different durations. Cyclic voltammetry (CV) was conducted to monitor

cellular $O_2^{\cdot-}$ and NO generation. SOD and NO synthase inhibitor were applied, respectively, to verify the $O_2^{\cdot-}$ and NO-caused current changes. Percentages of peak current enhancement in comparison with the control cells were used to evaluate the release of the analysts.

Fluorescent analysis of intracellular oxidative stress and mitochondrial membrane potential

$A375^{BRAFV600E}$ and $MV3^{BRAFV600E\ WT}$ cells were seeded at a density of 5×10^5/well in 6-well plates. PLX4032-challenged melanoma cells with/without SOD and NO synthase inhibitor treatments were stained with DCFH-DA and DAF-FM-DA, respectively. The cells were imaged under a fluorescence microscope (IX-71, Olympus Corp., Tokyo, Japan). NIH Image J software was used to analyze the fluorescence intensity.

Mitochondrial membrane potentials were measured with the JC-1 staining assay. PLX4032–treated cells were incubated with JC-1 (1:1000 dilution) for 20 min at 37°C. After washing with MOPS, the cells were observed under a fluorescence microscope with the red fluorescence (550 nm excitation/600 nm emission) and green fluorescence channels (485 nm excitation/535 nm emission). NIH Image J software was used to analyze the data and evaluate the change of fluorescence intensity.

Statistical analysis

Results were analyzed with the Student's *t*-test using an Origin Statistic software (OriginLab Corporation, USA). *p*-value < 0.05 was considered to be statistically significant. All experiments were performed three times in triplicates independently.

Results and discussion

Growth inhibition induced by PLX4032

Since PLX 4032 specifically targets melanoma cells containing $BRAF^{V600E}$ mutation, its influences on the growth of $A375^{BRAFV600E}$ and $MV3^{BRAFV600E\ WT}$ cells were examined to explore the optimal dosage. It is observed that PLX4032 inhibits the growth of $BRAF^{V600E}$ mutant melanoma cell line A375 in a dose-dependent manner (Fig. 1A). As the concentration of PLX4032 increases from 0 to 20 μM, the inhibition percentage enhances from 0% to around 60%. However, PLX4032 has no significant influence on the BRAFWT cell line MV3 even at the concentration as high as 20 μM. The results demonstrate the excellent specificity and efficiency of PLX4032 to $BRAF^{V600E}$ mutants. Because 5 μM PLX4032 can cause a 40% growth inhibition of $A375^{BRAFV600E}$ cells, it was selected as the optimal dosage for following experiments.

Extracellular lactate dehydrogenase (LDH) activity is widely applied to evaluate cell membrane integrity and cytotoxicity. The extent of cellular injury was estimated by the leakage of LDH from PLX4032-treated cells in this study (Fig.1B). In comparison with the control cells, LDH released from $A375^{BRAFV600E}$ cells increases 30%, 57% and 48% after 24, 48 and 72 h of PLX4032 treatment, respectively. However, under the same conditions, the changes in LDH leakage are negligible for $MV3^{BRAFV600E\ WT}$ cells. The significant leakage of LDH from A375 cells may indicate that PLX4032 could damage plasma membrane, thus leading to the death of the cells.

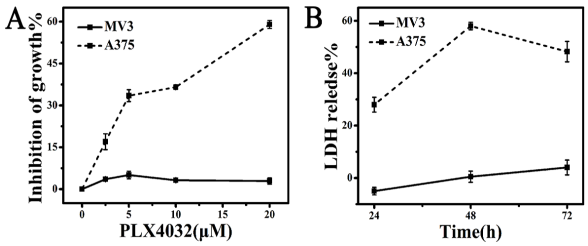

Fig.1 (A) PLX4032 induced growth inhibition in melanoma cell $A375^{BRAFV600E}$ and $MV3^{BRAFV600E\ WT}$ (MTT assay); (B) Lactate dehydrogenase (LDH) leakage from PLX4032-treated cells (LDH assay).

$O_2^{\cdot-}$ and NO production from PLX-4032-treated $A375^{BRAV600E}$ cell quantified by electrochemical sensors

Electrochemical sensors were employed in this study to monitor the $O_2^{\cdot-}$ and NO release from the untreated and PL4032-treated cells. $O_2^{\bullet-}$ is *in situ* generated for sensor characterization and calibration by adding KO_2 into PBS.[33] CV was performed in 0.1 M phosphate buffer solution (PBS, pH 7.4) to verify the performance of the as-prepared $O_2^{\cdot-}$ and NO sensors. Addition of 100 nM KO_2 induces a great enhancement of the oxidative peak current at around 0.7 V (blue line of Fig. 2A). After an introduction of SOD the increased peak current returns back to the baseline level (red line of Fig. 2A) due to the dismutation of $O_2^{\bullet-}$. For NO detection, an oxidative peak at 0.85 V appears in a testing system containing 0.25 mM NO (blue line of Fig. 2C). Hemoglobin (1.5 mM), which can disarm NO bioactivity[35], sharply decreases the characteristic NO peak (red line of Fig. 2C). The findings show that the nanomaterial-functionalized electrodes can be used to specifically sense $O_2^{\bullet-}$ and NO. To further demonstrate the detection sensitivity of the sensors, amperometric responses were measured by assaying serial concentration values of $O_2^{\cdot-}$ and NO. The $O_2^{\cdot-}$ electrochemical sensor possesses a fast response of 5 s to $O_2^{\cdot-}$ with a dynamic range from 10 to 200 nM. The corresponding calibration curve shows a detection limit of 2.5 nM and a sensitivity of 3.95 nA/nM (Fig. 2B, insert). A response time of 4 s against NO was achieved for the NO sensor (Fig.2D), which has a detection range from 0.2 to 4 μM, a detection limit of 28.17 nM and the sensitivity of 0.069 μA/μM.

$O_2^{\cdot-}$ generation from $A375^{BRAFV600E}$ and $MV3^{BRAFV600E\ WT}$ cells incubated with/without PLX4032 were measured using the as-prepared $O_2^{\cdot-}$ sensor. CV curves were collected to detect $O_2^{\cdot-}$ from PLX4032-treated $A375^{BRAFV600E}$ and $MV3^{BRAFV600E\ WT}$ cells. Changes of peak current intensity compared to control cells (without PLX4032 treatment) were plotted against drug treatment duration to reflect the $O_2^{\cdot-}$ secretion. As being shown in Fig. 3, 2, 4 and 8 h of PLX4032 incubations induce an increase of 24±1.2%, 22±0.9% and 21±0.7% in $O_2^{\cdot-}$generation from $A375^{BRAFV600E}$ cells, respectively (red dash line). While for $BRAF^{V600E}$ wide type MV3 cells, an about 10% increase of $O_2^{\cdot-}$generation is discovered after a 2-hour incubation with PLX4032 and the $O_2^{\cdot-}$ level remains constant from 4 to 24 h (black dash line). Interestingly, the $O_2^{\cdot-}$ release greatly decreases after 10 h and reaches the normal level after 24 h in $A375^{BRAFV600E}$ cells. This phenomenon may be possibly caused by the growth inhibition and cytotoxicity of PL4032. To prove the elevated current changes are indeed caused by PLX4032-triggered $O_2^{\cdot-}$ production, SOD (7.5 U/mL), a superoxide scavenger, was added in the cell

testing systems together with PLX4032. Results show that there is no significant change on the current intensity in both PLX4032-treated A375^{BRAFV600E} and MV3 $^{BRAFV600E\ WT}$ cells (solid lines in Fig.3). Therefore, the PLX4032 inhibitor can trigger the generation of $O_2^{\cdot-}$ from cells with BRAF^{V600E} mutation in an acute phase.

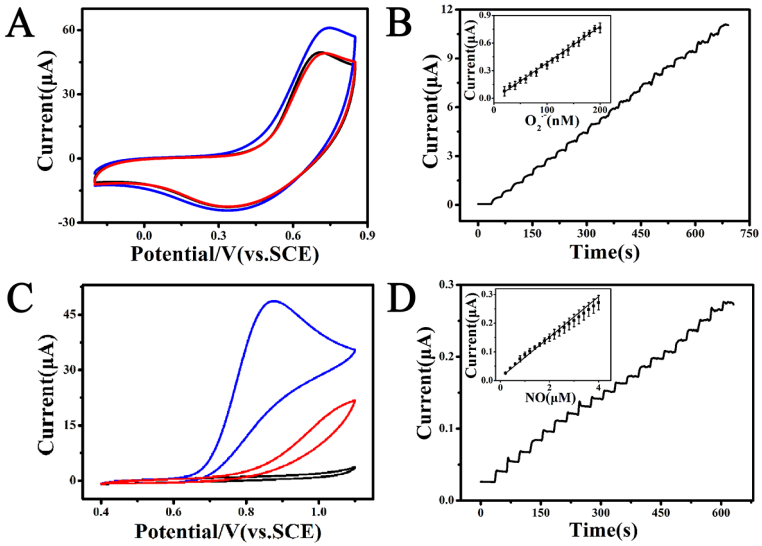

Fig. 2 (A)DNA-$Mn_3(PO_4)_2$–CNT modified glass carbon electrode for $O_2^{\cdot-}$detection. Cyclic voltammetry curves measured in PBS (black line), PBS + 100 nM KO_2 (blue line) and PBS + 100 nM KO_2 + superoxide dismutase (red line); (B) Amperometric response (*i-t* curve) and calibration curve for a serial concentration of KO_2; (C) rGO-CeO_2 modified glass carbon electrode for NO detection. Cyclic voltammetry curves measured in PBS (black line), PBS + 250 μM NO (blue line) and PBS + 250 μM NO + haemoglobin (red line); (D) Amperometric response (*i-t* curve) and calibration curve for a serial concentration of NO.

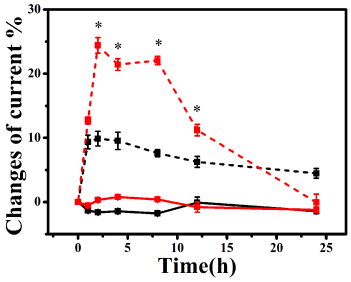

Fig.3 Effects of PLX4032 treatment on $O_2^{\cdot-}$generation from A375^{BRAFV600E} and MV3$^{BRAFV600E\ WT}$ cells. * denotes $p<0.05$; red dash line: PLX4032-treated A375^{BRAFV600E} cells, black dash line: PLX4032-treated MV3$^{BRAFV600E\ WT}$ cells, red solid line: PLX4032-treated A375^{BRAFV600E} cells incubated with superoxide dismutase, black solid line: PLX4032-treated MV3$^{BRAFV600E\ WT}$ cells incubated with superoxide dismutase.

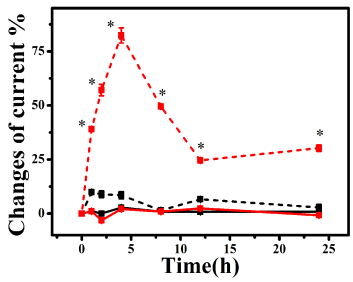

Fig.4 Effects of PLX4032 treatment on NO production of A375^{BRAFV600E} and MV3$^{BRAFV600E\ WT}$ cells. * denotes $p<0.05$, red dash line: PLX4032-treated A375^{BRAFV600E} cells, black dash line: PLX4032-treated MV3$^{BRAFV600E\ WT}$ cells, red solid line: PLX4032-treated A375^{BRAFV600E} cells incubated with NO synthase inhibitor, black solid line: PLX4032-treated MV3$^{BRAFV600E\ WT}$ cells incubated with NO synthase inhibitor.

Effects of PLX4032 on NO production from A375^{BRAFV600E} and MV3$^{BRAFV600E\ WT}$ cells were investigated with the calibrated NO sensor. Alterations of CV peak current intensity at 0.85 V, which is a characteristic peak of NO, were recorded to analyze changes of the NO level. During the first 4 h PLX4032 treatment triggers a sharp release of NO from A375^{BRAFV600E} cells. As the incubation time extends the extracellular NO level reduces and finally maintains at a relative constant level. Differently, changes of extracellular NO level of PLX4032-challenged MV3$^{BRAFV600E\ WT}$ cells are confined in a narrow range, which is significantly lower than those in A375^{BRAFV600E} cells (Fig.4). NG-monomethyl-L-arginine, monoacetate salt (L-NMMA, 0.1 mM), a nitric oxide synthase inhibitor, inhibits the PLX4032-induced NO production from A375 ^{BRAFV600E} cells. The results indicate that PLX4032 could specifically induce the production of NO in A375^{BRAFV600E} cells.

Increased intracellular ROS and NO in PLX4032-treated A375^{BRAFV600E} cells measured by fluorescent labeling

To confirm the participation of ROS in PLX4032-induced cell damage, DCFH-DA and DAF-FM-DA[11] were used to measure intracellular ROS and NO levels in melanoma cells. PLX4032 elevates the intracellular ROS level in A375^{BRAFV600E} cells as being evidenced by the strong fluorescent signal (Fig.5A). However, the treated MV3$^{BRAFV600E\ WT}$ cells demonstrate a negligible change of green fluorescence. The use of SOD fades the fluorescence caused by PLX4032 in A375^{BRAFV600E} cells. Quantitative analysis of the fluorescent images (Fig.5B) shows that the fluorescent intensity of PLX4032-challenged A375^{BRAFV600E} cells is significantly higher than that of other groups, indicating that PLX4032 specifically elevates the intracellular ROS level. Impacts of PLX4032 on intracellular NO generation from A375^{BRAFV600E} and MV3$^{BRAFV600E\ WT}$ cells were

also investigated with a fluorescent staining assay (Fig.6). PLX4032-incubated A375^{BRAFV600E} cells exhibit a very strong fluorescence, which can be removed by the application of L-NMMA (Fig.6A), suggesting the NO induction capability of PLX4032 in A375^{BRAFV600E} cells. In agreement with the findings in electrochemical measurements, the intracellular fluorescent assays reveal that PLX4032 could selectively induce the generation of ROS and NO in BRAF^{V600E} mutation positive melanoma cells.

Increased $O_2^{\cdot-}$ and NO production is associated with PLX 4032-induced cell damage

To investigate the role of $O_2^{\cdot-}$and NO in PLX 4032-induced cell damage, SOD and L-NMMA were used to treat the PLX4032-challenged cells in the MTT assay. As being shown in Fig. 7A, both SOD (7.5 U/mL) and L-NMMA (0.1 mM) can mitigate PLX4032-induced cell growth inhibition and cytotoxicity in A375^{BRAFV600E} cells. ROS are well recognized molecules that are involved in a variety of biochemical and pathological processes. $O_2^{\cdot-}$ can react with NO to form ONOO−, which may cause changes in the catalytic activity of enzymes and impair cell signal transduction.[24] Based on the data, it can be speculated that PLX4032 may stimulate the generation of $O_2^{\cdot-}$ and NO to break the intracellular oxidative balance, finally leading to cell damage.

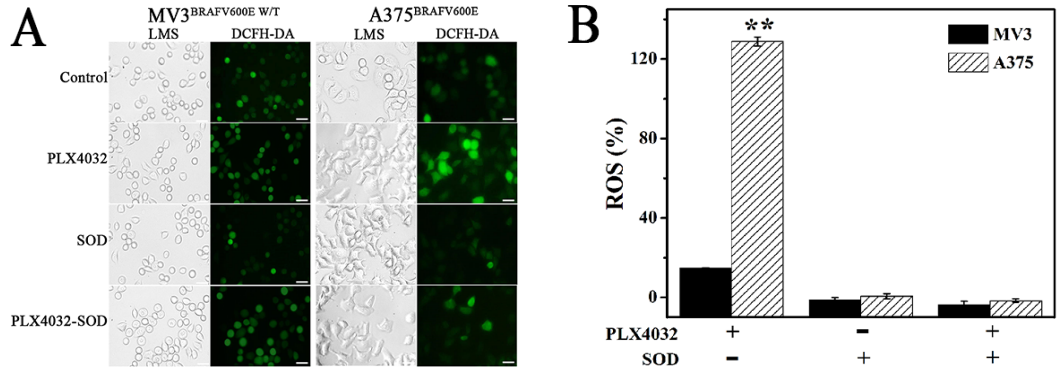

Fig. 5(A) DCFH-DA fluorescein staining of intracellular reactive oxygen species (ROS) generation from melanoma cells after an 8-h PLX4032 incubation (scale bar: 50 μm); (B) histogram of increased green florescent intensity compared with cells without PLX4032 treatment (n=3, ** denotes p<0.01). SOD: superoxide dismutase

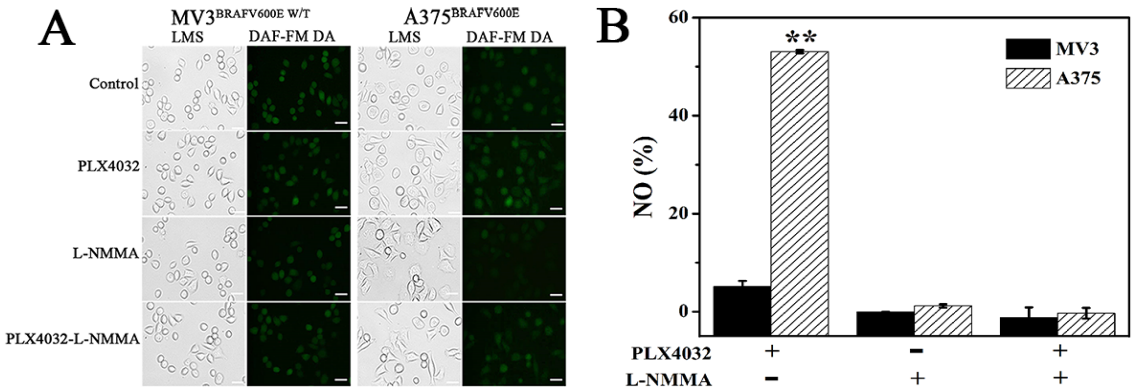

Fig.6 (A) DAF-FM-DA fluorescein staining of intracellular NO generation from melanoma cells after an 8-h PLX4032 incubation (scale bar: 50 μm); (B) histogram of increased green florescent intensity compared with cells without PLX4032 treatment (n=3, ** denotes p<0.01). L-NMMA: NG-monomethyl-L-arginine monoacetate

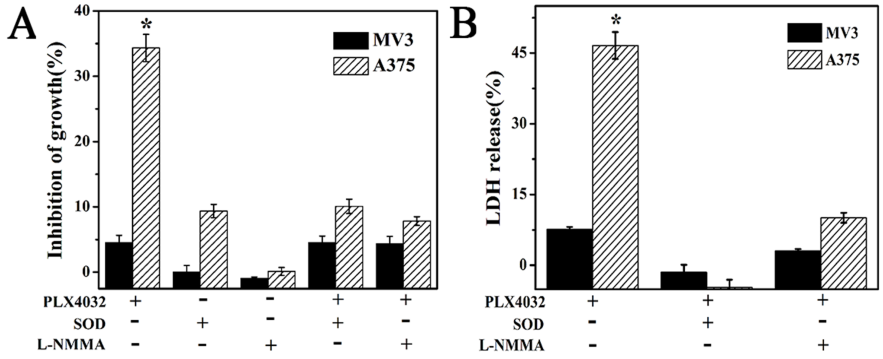

Fig.7(A) Effects of superoxide dismutase (SOD) and nitric oxide synthase inhibitor L-NMMA on PLX4032-induced growth inhibition of $A375^{BRAFV600E}$ and $MV3^{BRAFV600E\ WT}$ melanoma cells; (B) Lactate dehydrogenase (LDH) leakage from PLX4032 treated cells (n=3, * p<0.05).

Since it has been verified that PLX4032 specifically triggers $O_2^{\cdot-}$ and NO production from BRAF inhibitor-sensitive $A375^{BRAFV600E}$ cells, they might further cause depolarization of mitochondrial membrane potential and subsequent impairment of oxidative phosphorylation. Fig. 8A shows the uptake of JC-1, a specific mitochondrial membrane potential fluorescent marker, by $A375^{BRAFV600E}$ and $MV3^{BRAFV600E\ WT}$ cells. An increase of green fluorescence signal can be discovered in PLX4032-treated $A375^{BRAFV600E}$ cells, but not $MV3^{BRAFV600E\ WT}$ cells. PLX4032-treated $A375^{BRAFV600E}$ cells have a significantly increased green/red fluorescence ratio, which can be reduced to the background level after SOD or L-NMMA incubation (Fig.8B). Since the shift of JC-1 fluorescence from red to green indicates the depolarization of mitochondria, PLX4032 can interrupt mitochondria membrane potential, eventually resulting in dysfunction of mitochondria, which is one of hallmark of programmed cell death.

According to ROS-induced ROS theory, damaged mitochondria produce more ROS, especially $O_2^{\cdot-}$, to initiate mitochondria-driven ROS propagation through an inter-mitochondria signaling network.[36] Therefore, PLX4032 treatment induces a marked elevation of ROS production and a significant reduction of mitochondrial membrane potential, eventually leading to leakage of LDH and cell death. Selective induction of oxidative stress from melanoma cells with $BRAF^{V600E}$ mutation could possibly be one of the mechanisms for PLX4032–caused cell proliferation inhibition, although further research works must be carried out to fully understand the biological processes.

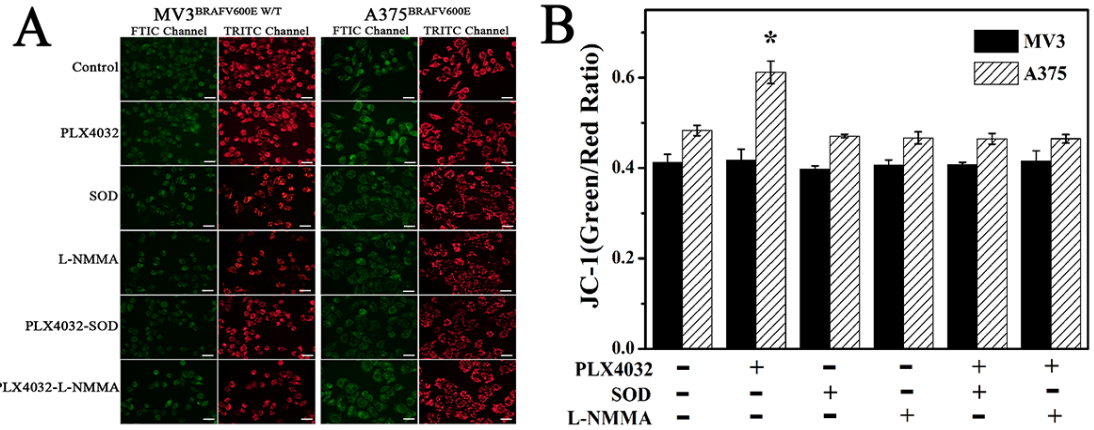

Fig. 8 (A) JC-1fluorescene staining of mitochondrial membrane potential from melanoma cells after an 8-h PLX4032 incubation (scale bar:50μm); (B) JC-1 green/red fluorescence ratio (n=3, * p<0.05). SOD: superoxide dismutase, L-NMMA: NG-monomethyl-L-arginine monoacetate.

Conclusions

The $BRAF^{V600E}$ inhibitor PLX4032 is an FDA-approved new drug for metastatic melanoma. It specifically inhibits the RAS/MEK/ERK signaling pathway that controls cell proliferation and adhesion. In the present study, electrochemical biosensors were fabricated to monitor $O_2^{\cdot-}$ and NO generation from PLX4032-treated melanoma cells. Results show that PLX4032 can specifically trigger the release of $O_2^{\cdot-}$ and NO from a $BRAF^{V600E}$ mutation A375 cell line, but not a $BRAF^{V600E}$ wild type MV3 cell line. Fluorescent analysis further shows that PLX4032 can selectively induce an increased intracellular ROS and NO levels in $A375^{BRAFV600E}$ cells. More importantly, incubation of $A375^{BRAFV600E}$ cell with SOD and NO synthase inhibitor can abolish PLX4032-initiated cell growth inhibition, proving the functions of $O_2^{\cdot-}$ and NO in PLX4032-caused cytotoxicity. Mitochondrial membrane potential has also been studied to verify the involvement of $O_2^{\cdot-}$and NO in the clinical activity of PLX4032. In summary, our study depicts that PLX4032 may elevate free radical production and secretion, leading to depolarization of mitochondrial membranes – potentially affecting proliferation of inhibitor-sensitive cells. It is proposed that selective induction of intracellular oxidative stress could possibly be one of the mechanisms for PLX4032–caused inhibition of melanoma cells harbouring $BRAF^{V600E}$ mutation. This work not only proposes a new mechanism for PLX4032-induced melanoma cell inhibition, but also highlights potential applications of electrochemical biosensors in cell biology and drug screening.

Notes

a Institute for Clean Energy & Advanced Materials, Faculty of Materials and Energy, Southwest University, Chongqing 400715, China
b Chongqing Key Laboratory for Advanced Materials and Technologies of Clean Energies, Chongqing 400715, China
c Chongqing Engineering Research Center for Rapid Diagnosis of Dread Disease, Southwest University, Chongqing, 400715, China
**Corresponding authors: Tel: +86-23-68254842; E-mail: lingyu12@swu.edu.cn (L. YU) and zslu@swu.edu.cn (Z.S. Lu)*

Acknowledgement

This work is financially supported by National Program on Key Basic Research Project of China (973 Program) under contract No.2013CB127804, Chongqing Key Laboratory for Advanced Materials and Technologies of Clean Energies, Start-up grant under SWU111071 from Southwest University, Chongqing International Collaboration Base for Science and Technology (Southwest University), Chongqing Engineering Research Center for Rapid diagnosis of Fatal Diseases, National Science

Foundation of China (No. 31200700 , 21375108) and Fundamental Research Funds for the Central Universities (XDJK20132013C059).

1. K. S. Smalley and K. T. Flaherty, *Br J Cancer*, 2009, **100**, 431-435.
2. B. B. Friday and A. A. Adjei, *ClinCancer Res*, 2008, **14**, 342-346.
3. L. Yu, E. Favoino, Y. Wang, Y. Ma, X. Deng and X. Wang, *Immunol Res*, 2011, **50**, 294-302.
4. V. Brower, *J Natl Cancer Inst*, 2010, **102**, 214-215.
5. J. A. Sosman, K. B. Kim, L. Schuchter, R. Gonzalez, A. C. Pavlick, J. S. Weber, G. A. McArthur, T. E. Hutson, S. J. Moschos, K. T. Flaherty, P. Hersey, R. Kefford, D. Lawrence, I. Puzanov, K. D. Lewis, R. K. Amaravadi, B. Chmielowski, H. J. Lawrence, Y. Shyr, F. Ye, J. Li, K. B. Nolop, R. J. Lee, A. K. Joe and A. Ribas, *N Engl J Med* 2012, **366**, 707-714.
6. D. H. Kim and T. Sim, *Arch Pharm Res*, 2012, **35**, 605-615.
7. E. W. Joseph, C. A. Pratilas, P. I. Poulikakos, M. Tadi, W. Wang, B. S. Taylor, E. Halilovic, Y. Persaud, F. Xing, A. Viale, J. Tsai, P. B. Chapman, G. Bollag, D. B. Solit and N. Rosen, *Proc Natl Acad Sci U S A*, 2010, **107**, 14903-14908.
8. M. Valko, D. Leibfritz, J. Moncol, M. T. Cronin, M. Mazur and J. Telser, *Int J Biochem Cell Bio*, 2007, **39**, 44-84.
9. M. Valko, C. J. Rhodes, J. Moncol, M. Izakovic and M. Mazur, *Chem-Biol Interact*, 2006, **160**, 1-40.
10. J. P. Fruehauf and F. L. Meyskens, Jr., *ClinCancer Res*, 2007, **13**, 789-794.
11. B. Kalyanaraman, V. Darley-Usmar, K. J. Davies, P. A. Dennery, H. J. Forman, M. B. Grisham, G. E. Mann, K. Moore, L. J. Roberts, 2nd and H. Ischiropoulos, *Free Radic Biol Med*, 2012, **52**, 1-6.
12. E. Bonfoco, D. Krainc, M. Ankarcrona, P. Nicotera and S. A. Lipton, *Proc Natl Acad Sci U S A*, 1995, **92**, 7162-7166.
13. D. Lobner, *J Neurosci Methods,* 2000, **96**, 147-152.
14. M. L. Marino, S. Fais, M. Djavaheri-Mergny, A. Villa, S. Meschini, F. Lozupone, G. Venturi, P. Della Mina, S. Pattingre, L. Rivoltini, P. Codogno and A. De Milito, *Cell Death Dis*, 2010, **1**, e87.
15. K. Irani and P. J. Goldschmidt-Clermont, *Biochem Pharmaco*, 1998, **55**, 1339-1346.
16. L. Wu and J. de Champlain, *Hypertension*, 1999, **34**, 1247-1253.
17. P. Corazao-Rozas, P. Guerreschi, M. Jendoubi, F. Andre, A. Jonneaux, C. Scalbert, G. Garcon, M. Malet-Martino, S. Balayssac, S. Rocchi, A. Savina, P. Formstecher, L. Mortier, J. Kluza and P. Marchetti, *Oncotarget*, 2013, **4**, 1986-1998.
18. A. Roesch, A. Vultur, I. Bogeski, H. Wang, K. M. Zimmermann, D. Speicher, C. Korbel, M. W. Laschke, P. A. Gimotty, S. E. Philipp, E. Krause, S. Patzold, J. Villanueva, C. Krepler, M. Fukunaga-Kalabis, M. Hoth, B. C. Bastian, T. Vogt and M. Herlyn, *Cancer cell*, 2013, **23**, 811-825.
19. N. Queisser, G. Fazeli and N. Schupp, *Biol Chem*, 2010, **391**, 1265-1279.
20. M. Ghasemi and A. Fatemi, *Neurosci Biobehav Rev*, 2014, **45C**, 168-182.
21. F. Murad, *Biosci Rep*, 2004, **24**, 452-474.
22. N. Liaw, J. M. Dolan Fox, A. H. Siddiqui, H. Meng and J. Kolega, *PloS one*, 2014, **9**, e101721.
23. A. C. Carr, M. R. McCall and B. Frei, *Arterioscler Thromb Vasc Biol*, 2000, **20**, 1716-1723.
24. P. Calcerrada, G. Peluffo and R. Radi, *Curr Pharm Des*, 2011, **17**, 3905-3932.
25. O. Myhre, J. M. Andersen, H. Aarnes and F. Fonnum, *Biochem Pharmacol*, 2003, **65**, 1575-1582.
26. H. M. Peshavariya, G. J. Dusting and S. Selemidis, *Free Radic Res*, 2007, **41**, 699-712.
27. H. Jiang, D. Parthasarathy, A. C. Torregrossa, A. Mian and N. S. Bryan, *J Vis Exp*, 2012, e3722.
28. L. Serrander, L. Cartier, K. Bedard, B. Banfi, B. Lardy, O. Plastre, A. Sienkiewicz, L. Forro, W. Schlegel and K. H. Krause, The Biochemical journal, 2007, 406, 105-114.
29. C. J. McNeil and P. Manning, *J Biotechnol*, 2002, **82**, 443-455.
30. F. Bedioui, D. Quinton, S. Griveau and T. Nyokong, *Phys Chem Chem Phys*, 2010, **12**, 9976-9988.
31. Z. Z. Shi, X. S. Wu, L. X. Gao, Y. L. Tian and L. Yu, *Anal Method*, 2014, **6**, 4446-4454.
32. C. X. Guo, X. T. Zheng, Z. S. Lu, X. W. Lou and C. M. Li, *Adv Mater*, 2010, **22**, 5164-5167.
33. S. C. Chang, N. Pereira-Rodrigues, J. R. Henderson, A. Cole, F. Bedioui and C. J. McNeil, *Biosens Bioelectron* 2005, **21**, 917-922.
34. X. Ma, W. Hu, C. Guo, L. Yu, L. Gao, J. Xie and C. M. Li, *Adv Mater*, DOI: 10.1002/adfm.201401443.
35. S. S. Gross and P. Lane, *Proc Natl Acad Sci U S A*, 1999, **96**, 9967-9969.
36. S. Marchi, C. Giorgi, J. M. Suski, C. Agnoletto, A. Bononi, M. Bonora, E. De Marchi, S. Missiroli, S. Patergnani, F. Poletti, A. Rimessi, J. Duszynski, M. R. Wieckowski and P. Pinton, *J Signal Transduct*, 2012, **2012**, 329635.

Graphic Abstract

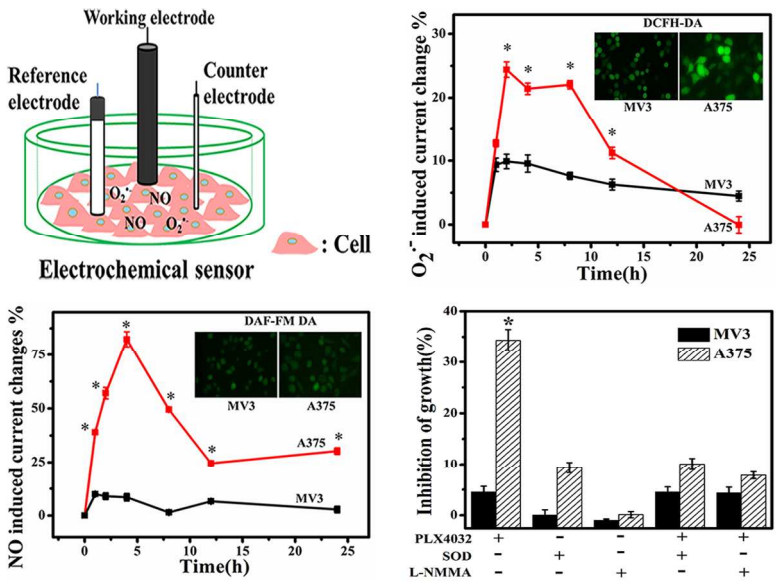

Electrochemical biosensors together with fluorescence staining were employed to monitor generation of superoxide and nitric oxide from PLX4032-treated cells.

Insight statement:

The $BRAF^{V600E}$ inhibitor PLX4032 (Vemurafinib) is an FDA-approved new drug for metastatic melanoma. In this study, an electrochemical biosensor together with conventional fluorescence staining techniques was employed to monitor extracellular and intracellular superoxide and nitric oxide of PLX4032-treated cells. Our findings suggest that PLX4032 may elevate free radical production and secretion, leading to depolarization of mitochondria membranes – potentially affecting proliferation of inhibitor-sensitive cells. Our findings further suggest that an interdisciplinary-modular approach to monitoring of cell free radical levels may be useful for cell biology and drug screening.